Environmental Science Processes & Impacts

ROYAL SOCIETY OF CHEMISTRY

PAPER

View Article Online
View Journal

Cite this: DOI: 10.1039/d2em00487a

Spatiotemporal patterns of soil heavy metal pollution risk and driving forces of increment in a typical industrialized region in central China†

Xue Yang[abc] and Yong Yang *[abc]

Excessive enrichment of soil heavy metals seriously damages human health and soil environment. Exploring the spatiotemporal patterns and detecting the influencing factors are conducive to developing targeted risk management and control. Based on the soil samples of Co, Cr, Cu, Mn, Ni, Pb, Zn, and Cd collected in one typical industrialized region in China from 2016 to 2019, this study analyzed the spatiotemporal pattern of geo-accumulation risk and potential ecological risk based on the spatiotemporal ordinary kriging (STOK) prediction, and probed the driving forces of heavy metal increments with the random forest (RF) regression model. The risk assessment revealed that soils were seriously contaminated by Pb, Cd, and Cu, moderately contaminated by Zn and Mn, and uncontaminated by Co, Cr, and Ni; more than 30% of areas had moderate to high potential ecological risks. From 2016 to 2019, soil heavy metal contents increased in more than 50% of regions and the growth rates of accumulations were ranked as Co (65%) > Ni (56%) > Mn (43%) > Pb (40%) > Cr (36%) > Zn (31%) > Cu (23%) > Cd (3%). High contents and increases of heavy metals in soils near industrial lands are higher. Smelter (24%), mine (20%), and factory (12%) were the major contributing factors for these heavy metal increments, followed by transportation (6%) and population (5%). The results indicated that the management of industrial discharge and contaminated soils should be strengthened to prevent the worsening soil heavy metal pollution in the study area.

Received 27th November 2022
Accepted 8th January 2023

DOI: 10.1039/d2em00487a

rsc.li/espi

Environmental significance

Soil heavy metal pollution is one of the major reasons for soil environment damage, especially in industrial regions due to rapid urbanization and industrialization development. The present study estimated the spatiotemporal distribution of soil heavy metal concentrations, assessed the pollution risks, and probed the driving forces of increments based on long-term soil sampling data in one typical industrialized region in China. This research revealed the spatiotemporal pattern of soil heavy metal pollution and the contributing sources of pollution increase, which provides the base for the prevention and control of soil heavy metal pollution.

1 Introduction

Soil heavy metal pollution is one of the major reasons for soil environment damage, and exposure to heavy metals may pose a health risk to human beings.[1] Soil heavy metal pollution is increasingly severe and in more urgent need of attention in China, especially in industrial regions due to rapid urbanization and industrialization development.[2,3] China's national communique of the soil pollution survey stated that the overstandard rate of soil heavy metals in industrial and mining regions was 33.4%.[4] Therefore, intensively monitoring the soil heavy metal pollution risk and exploring the pollution sources are necessary for the prevention and control of soil pollution.

Thus far, many studies developed a pollution risk assessment of soil heavy metals based on the current investigation.[5–9] In accordance with different pollution risk indices (*e.g.*, geo-accumulation index and ecological risk index), these studies analyzed the spatial pattern of the soil heavy metal cumulation degree and integrated pollution risks, and identified the regions under priority control. Moreover, some researchers also explored the contribution of pollution sources and heavy metal to pollution risk under different land uses by combining risk assessment indices and source apportionment methods, which quantitatively revealed the contributing sources and spatial heterogeneity of soil heavy metal pollution risks.[10–12] However, soil heavy metal pollution

[a]College of Resources and Environment, Huazhong Agricultural University, Wuhan 430070, China
[b]Key Laboratory of Arable Land Conservation (Middle and Lower Reaches of the Yangtze River), Ministry of Agriculture, China
[c]Hubei Key Laboratory of Soil Environment and Pollution Remediation, Wuhan, China

† Electronic supplementary information (ESI) available. See DOI: https://doi.org/10.1039/d2em00487a

usually has temporal variation due to its enrichment, diffusion, and the influence of anthropogenic activities.[13,14] Thus, only monitoring the spatiotemporal pattern of soil heavy metals can provide more valid recommendations for pollution control.

The spatiotemporal prediction of soil heavy metal pollution is the key step to realize dynamic monitoring, but it received less attention due to its high cost and long-term labor-intensive implementations. Jiang *et al.*[13] used ordinary kriging to explore the spatiotemporal variation of soil heavy metals in 1983 and 2010 in the Poyang Lake region of China. He *et al.*[15] employed the inverse distance weight method to probe the temporal changes of soil heavy metal distribution in 2011 and 2016 in Wenling. Taghizadeh-Mehrjardi *et al.*[16] used the random forest (RF) model with multiple environmental variables to predict the spatial distribution of soil heavy metals in the Yazd Province of Iran in 1986, 1999, 2010, and 2016. The above studies all used spatial prediction methods because of their attention only on the soil heavy metal pollution in several discontinuous periods, and these methods have high requirement for the spatial distribution of soil samples in each period. Although the application of auxiliary data can improve the accuracy of spatial prediction to a certain extent, collecting contemporaneous environmental data completely is difficult due to the limitations of the regional scale and research period. Spatiotemporal ordinary kriging (STOK) is a spatiotemporal geostatistical method based on the temporal and spatial variations of the estimated attribute.[17] Because of its higher convenience and independence from auxiliary data, STOK has been extensively used in predicting the spatiotemporal distribution of various environmental properties, such as water nitrogen,[18] precipitation,[19] and soil organic matter.[20] In the absence of auxiliary data, whether it can better estimate the spatiotemporal distribution of heavy metals only based on soil samples needs to be explored. Thus, STOK is employed to explore the spatiotemporal pattern of regional soil heavy metal pollution in the present study.

Another focused study is to explore the driving forces of soil heavy metals, which is useful for understanding the pollutant sources and controlling pollution. To date, numerous studies found that soil heavy metal pollution results from multiple environmental variables, for example, soil properties, vegetation, socioeconomic factors, agriculture production, transportation, and industrial activities.[21–23] However, few studies paid attention to the environmental effects on soil heavy metal increments. Analyzing the driving factors for heavy metal contents can reveal the pollution sources with a long-term effect, whereas analyzing the driving factors for heavy metal increments can reveal the pollution sources with a short-term effect. Compared with the former, the latter is more instructive for the management and control of soil heavy metal pollution deterioration in one short period.

With the development of the stochastic simulation technique, the RF model has gradually been applied to the driving mechanism analysis. RF is a commonly used data mining algorithm based on machine learning theory, and has an outstanding ability to capture nonlinear relationships and insensitivity to outliers.[24] It has been increasingly employed to probe the driving forces of various environmental pollutants because it can provide a deeper understanding of predictor contributions and more accurately identify the dominant factors.[23,25,26] Based on the above background, this study employed the RF model to explore the contributing factors for soil heavy metal increments.

In view of the above considerations, taking a typical industrialized area in central China as the study area, we investigated the soil Co, Cr, Cu, Mn, Ni, Pb, Zn, and Cd pollution from 2016 to 2019. The objectives of this study were as follows: (a) to estimate the spatiotemporal distribution of soil heavy metal contents with STOK, (b) to assess the soil heavy metal pollution risks, and (c) to analyze the driving forces of heavy metal increments. The results will provide the spatiotemporal dynamic pattern of soil heavy metal pollution risks and information regarding the contributing sources for heavy metal increments, which are useful for controlling heavy metal pollution and protecting the soil environment in the industrial area.

2 Materials and methods

2.1 Study area and soil sample collection

The study area is one typical industrialized area located in central China, which has a total area of 184.68 km^2. In accordance with the remote sensing image interpretation and field survey, the main types of land use in the study area are paddy (23%), mountain and forest (18%), dry land (17%), urban (11%), and the total percentage of industrial and mining land (including factory, mine, and smelter) is approximately 11%. A total of 829 topsoil samples (0–20 cm depth) were collected from 2016 to 2019 to monitor the spatiotemporal pattern of soil heavy metal pollution (Fig. 1). All soil samples were air-dried in a room and passed through a 100-

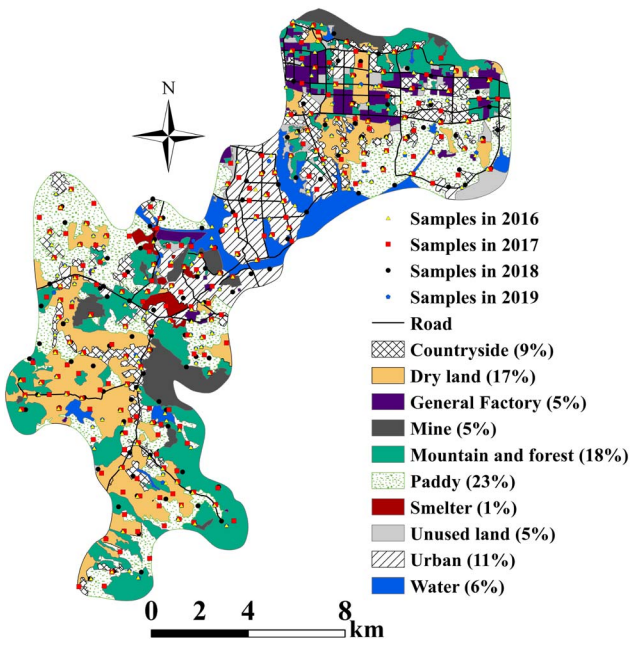

Fig. 1 Spatial distribution of soil samples from 2016 to 2019, roads and land use in the study area.

mesh polyethylene sieve, and the milled samples were used to analyze the heavy metal concentration. About 0.20 g of each sample was weighed in a digestion vessel, and 8 ml HNO_3 and 2 ml HF were added for microwave digestion. The concentrations of Co, Cr, Cu, Mn, Ni, Pb, Zn, and Cd were determined by inductively coupled plasma-mass spectrometry. The analysis precision was controlled by checking the reagent blanks and standard reference materials (GBW07403, the National Research Center for Certified Reference Materials of China). The recoveries of samples spiked with standards of all elements were about 91–112%, indicating a good accuracy of the analytical method. In this study, the sample was acceptable when the relative standard deviation of the duplicate samples was within 10%. The calibration curves of each element were constructed by using the linear regression model based on mixed standard solutions, and the correlation coefficients of the curves were all larger than 0.9999. The limit of detection (LOD) values of Co, Cr, Cu, Mn, Ni, Pb, Zn, and Cd are 0.12, 0.61, 0.27, 0.36, 0.14, 0.31, 1.00, and 0.01 mg L^{-1}, respectively, and the limit of quantification (LOQ) values are 0.42, 2.03, 0.90, 1.18, 0.48, 1.02, 3.33, and 0.04 mg L^{-1}, respectively.

2.2 Spatiotemporal prediction of soil heavy metals

The soil heavy metal content is an environmental attribute distributed continuously in space and time dimensions. Thus, the soil heavy metal content can be defined based on the space-time random field as $C(\boldsymbol{p}) = \{C:\boldsymbol{p} = (\mathbf{s}, t), \mathbf{s} = (s_1, s_2) \in S, t \in T\}$, where $C(\boldsymbol{p})$ is the value of the soil heavy metal concentration at space-time point $\boldsymbol{p}$ with space domain $S(S \subset R^2)$ and time domain $T(T \subset R)$, $\mathbf{s}$ is the spatial coordinate, and t is the time. Based on the space-time random field, STOK is conducted through the following steps.

First, the empirical spatiotemporal semi-variogram is calculated to characterize the spatiotemporal variation of soil heavy metal concentrations.[27] The empirical spatiotemporal semi-variogram is calculated by using eqn (1), where h_S and h_T are the space and time lags, respectively, and $N(h_S, h_T)$ is the number of pairs of points with the space lag (h_S) and time lag (h_T).

$$\widehat{\gamma}(h_S,\ h_T) = \frac{1}{2N(h_S,\ h_T)} \sum_{i=1}^{N(h_S,h_T)} [C(s_i,\ t_i) - C(s_i + h_S,\ t_i + h_T)]^2 \quad (1)$$

Then, the theoretical spatiotemporal semi-variogram model is simulated. The temporal variation characteristics of soil heavy metal concentrations are complex due to the spatiotemporal change of their source and soil environment. To obtain the theoretical spatiotemporal semi-variogram with higher quality, two functions were used to simulate the theoretical semi-variogram of soil heavy metal pollution, as shown in eqn (2) and (3). Eqn (2) is a spatiotemporal non-separable variogram model and is suitable for the spatiotemporal semi-variogram without remarkable fluctuation at space and time scales. Eqn (3) is a spatiotemporal separable variogram model and is suitable for a spatiotemporal semi-variogram with remarkable fluctuation in the time scale.

$$\gamma(h_S,\ h_T) = C_0 + C\left[1 - \left(1 + \frac{1}{w^2}(h_S + \alpha h_T)^2\right)^{-\frac{v}{2}} e^{-\frac{1}{\xi}|h_S + \alpha h_T|}\right] \quad (2)$$

$$\gamma(h_S,\ h_T) = C_0 + C_1\left[1 - \left(1 - e^{\left(-\frac{h_S}{\lambda}\right)}\right)\right] + C_2\left[1 - \left(1 - e^{\left(-\frac{h_T}{\mu}\right)}\right)\right]\cos\left(\frac{2\pi h_T}{\rho}\right) \quad (3)$$

Finally, the theoretical spatiotemporal semi-variogram is used to generate the weights of neighboring points by solving matrix eqn (4),[19] where $\gamma(\boldsymbol{p}_i, \boldsymbol{p}_j)$ is the theoretical spatiotemporal semi-variogram between points $\boldsymbol{p}_i$ and $\boldsymbol{p}_j$, and λ_i is the weight of sample point $\boldsymbol{p}_i$ for the estimated point $\boldsymbol{p}_0$. The soil heavy metal content of the estimated point $C_{\boldsymbol{p}_0}$ is calculated by using eqn (5), where λ_i and $C_{\boldsymbol{p}_i}$ are the weight and heavy metal content of the neighboring sample point $\boldsymbol{p}_i$, respectively. In this study, the cell size of grid data for soil heavy metal concentrations is 100 m × 100 m × 1 year, and the number of grids is 18 997 × 4 years.

$$\begin{bmatrix} \gamma(\boldsymbol{p}_1,\ \boldsymbol{p}_1) & \gamma(\boldsymbol{p}_1,\ \boldsymbol{p}_2) & \cdots & \gamma(\boldsymbol{p}_1,\ \boldsymbol{p}_n) & 1 \\ \gamma(\boldsymbol{p}_2,\ \boldsymbol{p}_1) & \gamma(\boldsymbol{p}_2,\ \boldsymbol{p}_2) & \cdots & \gamma(\boldsymbol{p}_2,\ \boldsymbol{p}_n) & 1 \\ \vdots & \vdots & \cdots & \vdots & \vdots \\ \gamma(\boldsymbol{p}_n,\ \boldsymbol{p}_1) & \gamma(\boldsymbol{p}_n,\ \boldsymbol{p}_2) & \cdots & \gamma(\boldsymbol{p}_n,\ \boldsymbol{p}_n) & 1 \\ 1 & 1 & \cdots & 1 & 0 \end{bmatrix} \times \begin{bmatrix} \lambda_1 \\ \lambda_2 \\ \vdots \\ \lambda_n \\ \mu \end{bmatrix} = \begin{bmatrix} \gamma(\boldsymbol{p}_1,\ \boldsymbol{p}_0) \\ \gamma(\boldsymbol{p}_2,\ \boldsymbol{p}_0) \\ \vdots \\ \gamma(\boldsymbol{p}_n,\ \boldsymbol{p}_0) \\ 1 \end{bmatrix} \quad (4)$$

$$C_{\boldsymbol{p}_0} = \sum_{i=1}^{n} \lambda_i C_{\boldsymbol{p}_i} \quad (5)$$

The spatiotemporal prediction accuracy is assessed by using the leave-one-out method, and the accuracy criteria include the r, mean average error (MAE), and root mean square error (RMSE) between the observed value and the predicted value.

2.3 Risk assessment of soil heavy metals

2.3.1 Geo-accumulation index (I_{geo}). The risk assessment of soil heavy metals was developed based on the spatiotemporal distributions of soil heavy metal concentrations. The geo-accumulation index (I_{geo}) has been widely applied to assess the contamination degree of a single heavy metal, and is defined as eqn (6),[28–30] where C_i is the concentration of heavy metal i, and

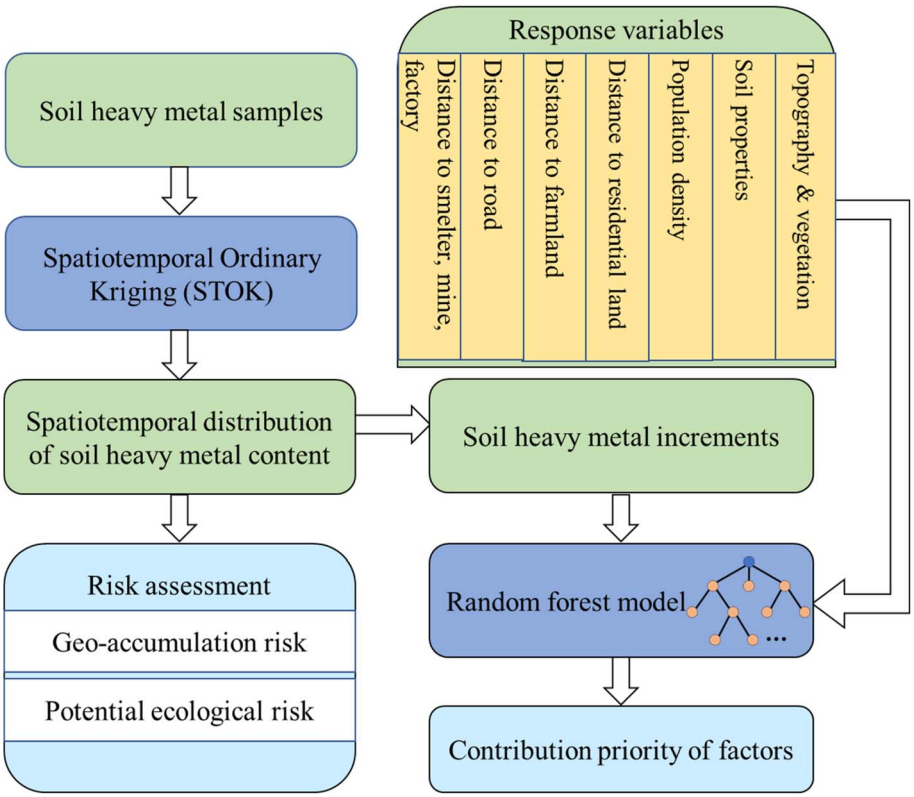

Fig. 2 Flow chart of methods in the study.

C_b is the geochemical background value of heavy metal in the province of the study area. The background values of the studied heavy metals are 15.4, 86, 30.7, 712, 37.3, 26.7, 83.6, and 0.17 mg kg^{-1} for Co, Cr, Cu, Mn, Ni, Pb, Zn, and Cd, respectively.[31] According to Müller,[32] I_{geo} is classified into seven classes: $I_{geo} \leq 0$, uncontaminated; $0 < I_{geo} \leq 1$, uncontaminated to moderately contaminated; $1 < I_{geo} \leq 2$, moderately contaminated; $2 < I_{geo} \leq 3$, moderately to heavily contaminated; $3 < I_{geo} \leq 4$, heavily contaminated; $4 < I_{geo} \leq 5$, heavily to extremely contaminated; and $I_{geo} > 5$, extremely contaminated.

$$I_{geo} = \log_2\left(\frac{C_i}{1.5C_{bi}}\right) \quad (6)$$

2.3.2 Potential ecological risk index (RI). Potential ecological risk index (RI) is used to evaluate the integrated risk degrees of soil heavy metals.[33] This index combines ecology, biochemistry, and other aspects to evaluate the potential ecological hazard of heavy metals.[34] This index is calculated as eqn (7), where EI_i is the single potential ecological risk index of heavy metal i, C_i is the concentration of heavy metal i, S_i is the environmental quality standard of heavy metal i, and T_i is the toxicity coefficient of heavy metal i. In this study, the background values of the studied heavy metals were used as the quality standard, and the toxicity coefficients of each heavy metal were Co = 5, Cr = 2, Cu = 5, Mn = 1, Ni = 5, Pb = 5, Zn = 1, and Cd = 30.[35] The potential ecological hazard posed by heavy metals was classified into four grades:[33] RI < 150, low ecological risk; 150 ≤ RI < 300, moderate ecological risk; 300 ≤ RI < 600, considerable ecological risk; RI ≥ 600, very high ecological risk.

$$RI = \sum_{i=1}^{n} EI_i = \sum_{i=1}^{n}\left(\frac{C_i}{S_i} \times T_i\right) \quad (7)$$

2.4 Driving forces of heavy metal increments

2.4.1 Driving factors. Soil heavy metal accumulation is influenced by diverse environmental factors, and the factors can be divided into natural factors and those related to anthropogenic activities.[36] Among the natural factors, soil properties, such as soil pH, cation exchange capacity (CEC), organic content, and soil thickness (ST), are critically important factors controlling the heavy metal migration ability in soils.[22,37,38] Topography and vegetation coverage have a remarkable effect on the heavy metal movement and accumulation in soil.[22,39] Human activities usually accelerate the soil heavy metal accumulation due to various production emissions. In particular, industrial activities (*e.g.*, mining and metal processing) highly influence soil heavy metal accumulation as well as the discharge of wastewater and waste gas.[40,41] Application of pesticides and traffic emissions also lead to higher soil heavy metal pollution.[42,43] Furthermore, residential land and population density were found to be highly correlated with the soil heavy metal accumulation pattern due to domestic discharge.[44]

In view of the above considerations, 14 factors were introduced to explore the driving forces of soil heavy metal increments, and their spatial distributions are shown in Fig. S1.† Soil pH, CEC, soil organic carbon (SOC), and ST were collected from the National Earth System Science Data Center, National Science and Technology Infrastructure of China (**https://www.geodata.cn**), and the year of these datasets was 2018. The elevation and slope were collected from the geospatial data cloud platform (**https://www.gscloud.cn/**), and the normalized difference vegetation index (NDVI) was the average annual NDVI from 2016 to 2019 collected from the National Aeronautics and Space Administration (**https://modis.gsfc.nasa.gov/**). The traffic road network was collected from the Bigmap platform (**https://www.bigemap.com/**) and used to generate the data of distance to traffic road. The population density was the average population density during 2016–2019 collected from the WorldPop platform (**https://www.worldpop.org/**). Land use data were obtained by using a field survey and remote sensing image interpretation, which was used to generate the data of distance to farmland, distance to smelter, distance to general factory, distance to mine, and distance to residential land. Notably, general factory is a factory except for the quarry and smelter, and mainly processes various products, such as electronic products, metal instruments, clothing, food, *etc.*

2.4.2 Random forest. The RF model proposed by Breiman[24] is a nonlinear nonparametric method based on machine learning theory. It consists of numerous decision trees, and each tree is trained by a set of variables randomly selected by bootstrap sampling at each node. In the RF algorithm, the number of decision trees and the number of variables used in the binomial tree are the two important input parameters related to the prediction accuracy. In this study, the RF regression algorithm was used to calculate the contributions of different variables for soil heavy metal increments generated with STOK and was implemented with the Python software package in Spyder software 4.2.5. The soil heavy metal increment from 2016 to 2019 was the dependent variable, and the natural and anthropogenic variables mentioned in Section 2.4.1 were entered as predictors in the RF algorithm. About 70% of the samples were used to train the trees, and 30% of the samples were used in the internal 10-fold cross-validation test to evaluate the RF performance. The number of decision trees and the number of variables were set to 500 and 1 to build the RF, respectively. The prediction accuracy of RF was evaluated with R^2 and mean squared error (MSE). The flow chart of all methods mentioned in Sections 2.2–2.4 is shown in Fig. 2.

3 Results

3.1 Descriptive statistics and spatiotemporal estimation of soil heavy metal concentrations

The statistics of 829 topsoil samples are shown in Table S1.† The average concentrations of Cu, Pb, Zn, and Cd are more than twice their background values. Soil Co, Cr, Mn, and Ni have moderate variability, whereas Cu, Pb, Zn, and Cd have strong variability.[45] Among the eight elements, the percentages of samples beyond the background values of Cu, Pb, Zn, and Cd are larger than 50% approximately, which indicates that the pollution of the four heavy metals are more serious than that of the other heavy metals.

The *K–S* values for the observed data are all less than 0.05, indicating that the studied heavy metal concentrations all display nonnormal distributions. To obtain the data following the normal distribution, the observed values of Co, Cr, Cu, Pb, Zn, and Cd were transformed by logarithm, and the observed values of Mn and Ni were transformed by square root. The *K–S* test values of the transformed data are slightly smaller or larger than 0.05, indicating that the transformed data of studied elements are close to the normal distribution. Based on the transformed data, the spatiotemporal empirical semi-variogram was calculated by using eqn (1), and the spatiotemporal theoretical semi-variogram was obtained by using eqn (2) and (3). In the study, the theoretical semi-variograms of Co, Cu, Ni, and Pb were simulated by using eqn (2), and those of Cr, Mn, Zn, and Cd were simulated by using eqn (3). The R^2 values of all theoretical variograms are larger than 0.7 (Fig. 3), which shows that the empirical semi-variogram is well fitted based on the two theoretical variogram forms. As shown in Fig. 3, the variogram of these heavy metals at the time and space dimensions are quite different. In terms of Co, Ni, and Pb, the variogram increases substantially with increasing space and time distances. The variogram of Cu is stable at the time distance, and increases with the increasing spatial distance until approximately 12 km. Different from those of Co, Cu, Ni and Pb, the variograms of Cr, Mn, Zn and Cd fluctuate considerably at the time distance and increase with the increasing spatial distance at 4, 10, 12, and 10 km approximately.

Based on the theoretical semi-variogram, the STOK was implemented to obtain the spatiotemporal distributions of heavy metal concentrations from 2016 to 2019 (Fig. S2†). As shown in Table S2,† the *r* values of these heavy metals are all larger than 0.5, indicating the higher estimation accuracy in the presence of strong spatiotemporal variability.

3.2 Spatiotemporal patterns of soil heavy metal pollution risk

Based on the spatiotemporal distribution of soil heavy metal concentrations, I_{geo} and RI were calculated by using eqn (6) and (7) to assess the degrees of cumulative pollution risk and ecological hazard. From 2016 to 2019, the average I_{geo} values of heavy metals are ranked as Cd (0.77) > Cu (0.76) > Pb (0.41) > Zn (−0.13) > Co (−0.80) > Mn (−0.81) > Cr (−1.32) > Ni (−1.33), which shows that the average accumulation degrees of Cu, Pb, and Cd are remarkably higher than that of the other heavy metals. The average greatest I_{geo} values are ranked as Cd (3.46) > Pb (3.01) > Cu (2.81) > Zn (1.37) > Mn (0.27) > Co (−0.08) > Ni (−0.45) > Cr (−0.67), indicating that the whole study region was not contaminated by Ni, Cr and Co, and some regions were moderately contaminated by Zn and Mn, and heavily contaminated by Cu, Pb, and Cd. Among the heavy metals with higher enrichment, Cu was highly enriched in the central area, while the spatial distribution patterns of Pb, Zn, and Cd were

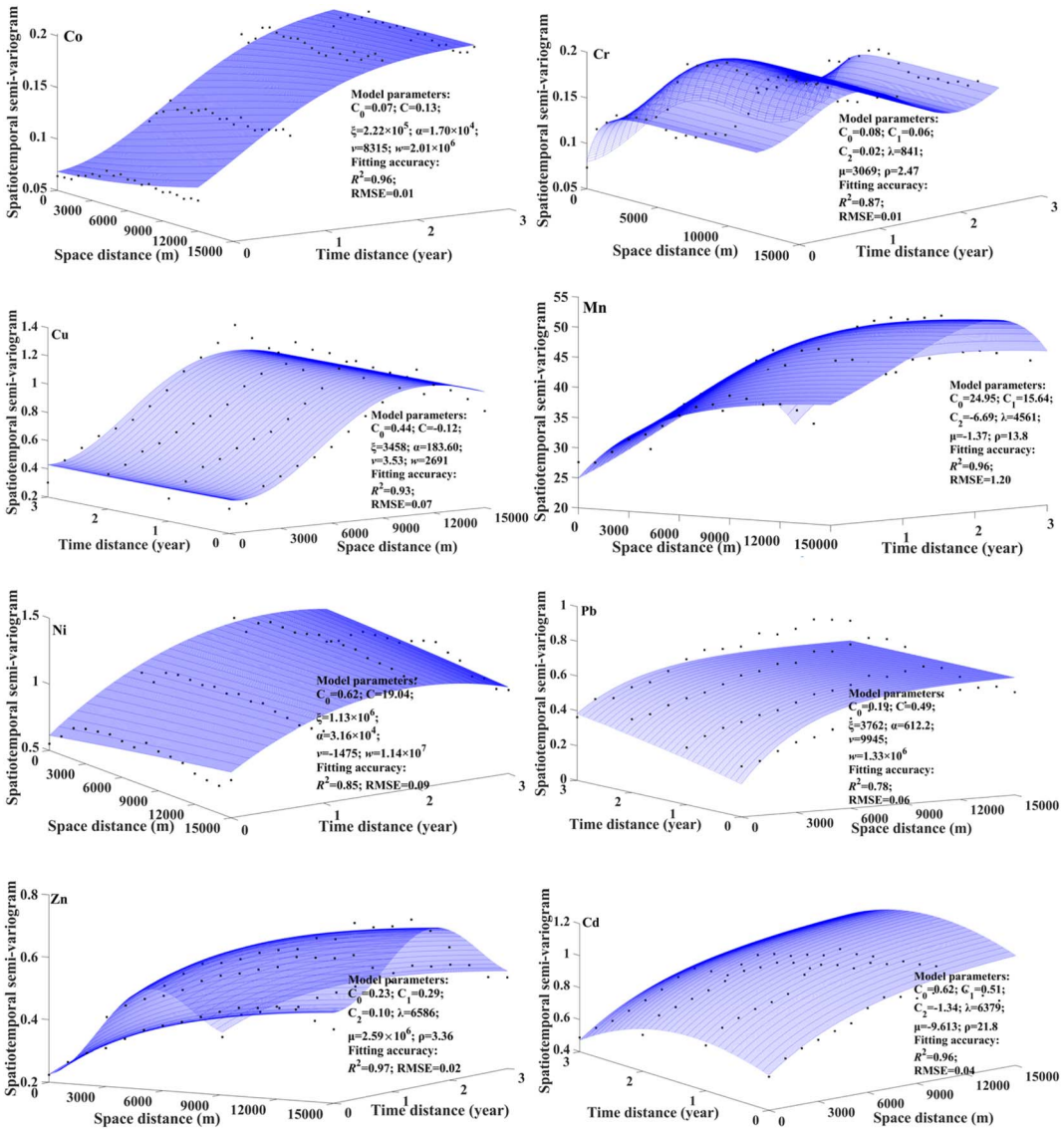

Fig. 3 Spatiotemporal semi-variogram of soil heavy metal concentrations. Scatters: experimental semi-variogram; surface: theoretical semi-variogram.

relatively similar, and their high enrichments were mainly in the central and northern areas (Fig. 4). As shown in Fig. S4,† there are several smelters, quarries, and mining lands in the central and north areas, which may lead to the high accumulations of soil Cu, Pb, Zn and Cd. In addition, although the enrichment degrees of most heavy metals had a substantial increasing trend, the areas with the highest enrichment changed slightly during 2016–2019.

The RI ranges from 28.59 to 604.92, indicating that the potential ecological risk level in the study area ranges from low ecological risk to very high ecological risk. The average contributions of the studied heavy metals are ranked as: Cd (67.61%) > Cu (12.31%) > Pb (9.31%) > Co (4.38%) > Ni (3.03%) > Zn (1.31%) > Cr (1.23%) > Mn (0.83%), which indicated that the potential ecological risk is mainly from soil Cd, Cu, and Pb. From 2016 to 2019, the contribution of Cd to RI had a slight decreasing trend, and the contributions of other heavy metals changed slightly (Fig. S3†). Due to the large contributions of Cd, Pb, and Cu, the spatial trend of the RI was extremely similar to that of these heavy metals. As shown in Fig. 4, the higher ecological risk is mainly located in the central area during 2016–2019, which is in accordance with previous studies.[10,46,47] As reported in these research studies, long-term industrial and mining activities in the central area caused severe soil heavy metal pollution.

Fig. 5 shows the percentages of different accumulation risk levels and the potential ecological risk levels in each year. The RI levels include low ecological risk, moderate ecological risk, considerable ecological risk, and very high ecological risk, and their annual average percentages are 66%, 28%, 4%, and 2%, respectively. The geo-accumulation risk levels of soil Co, Cr, Mn, and Ni in most areas are uncontaminated, and those of Zn are uncontaminated, uncontaminated to moderately contaminated, and moderately contaminated with annual average

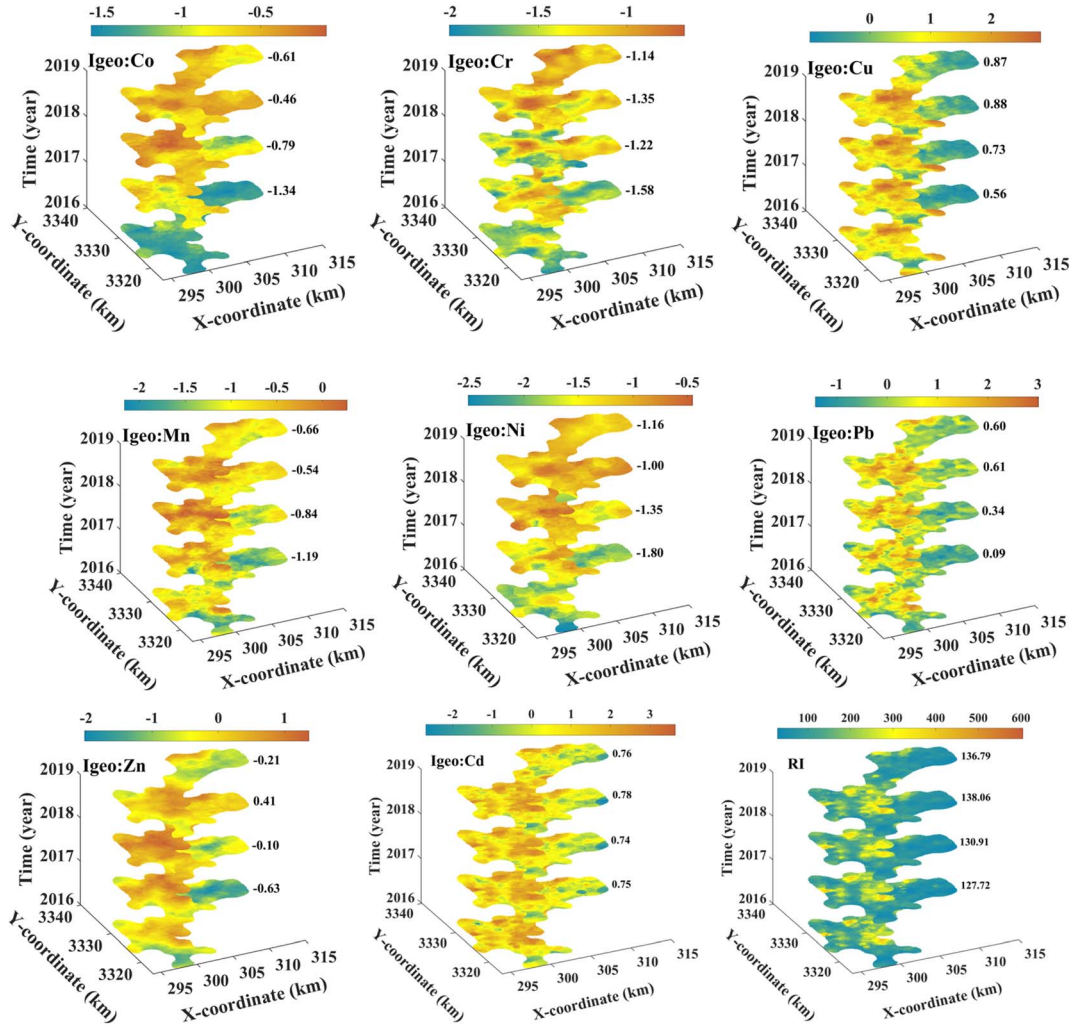

Fig. 4 Spatial distributions of geo-accumulation risk and potential ecological risk from 2016 to 2019.

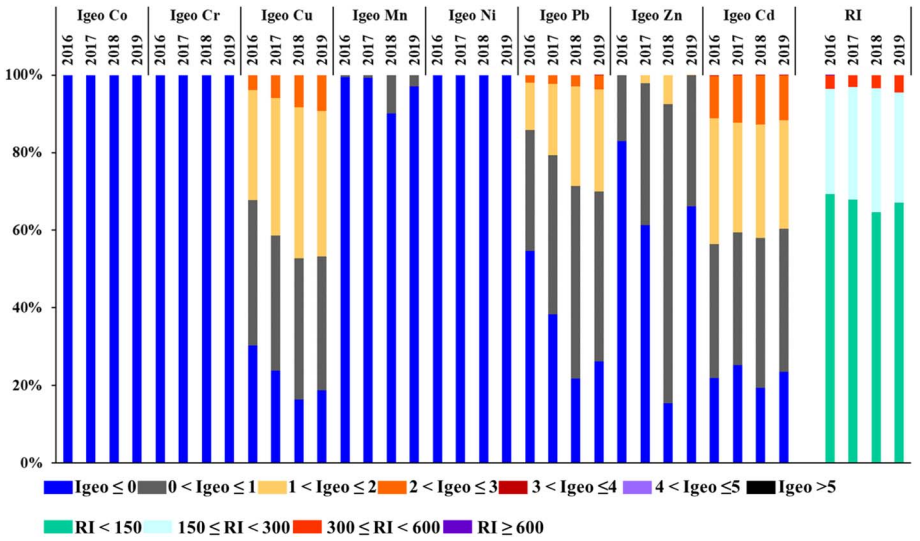

Fig. 5 Percentages of different levels of geo-accumulation risk and potential ecological risk in each year.

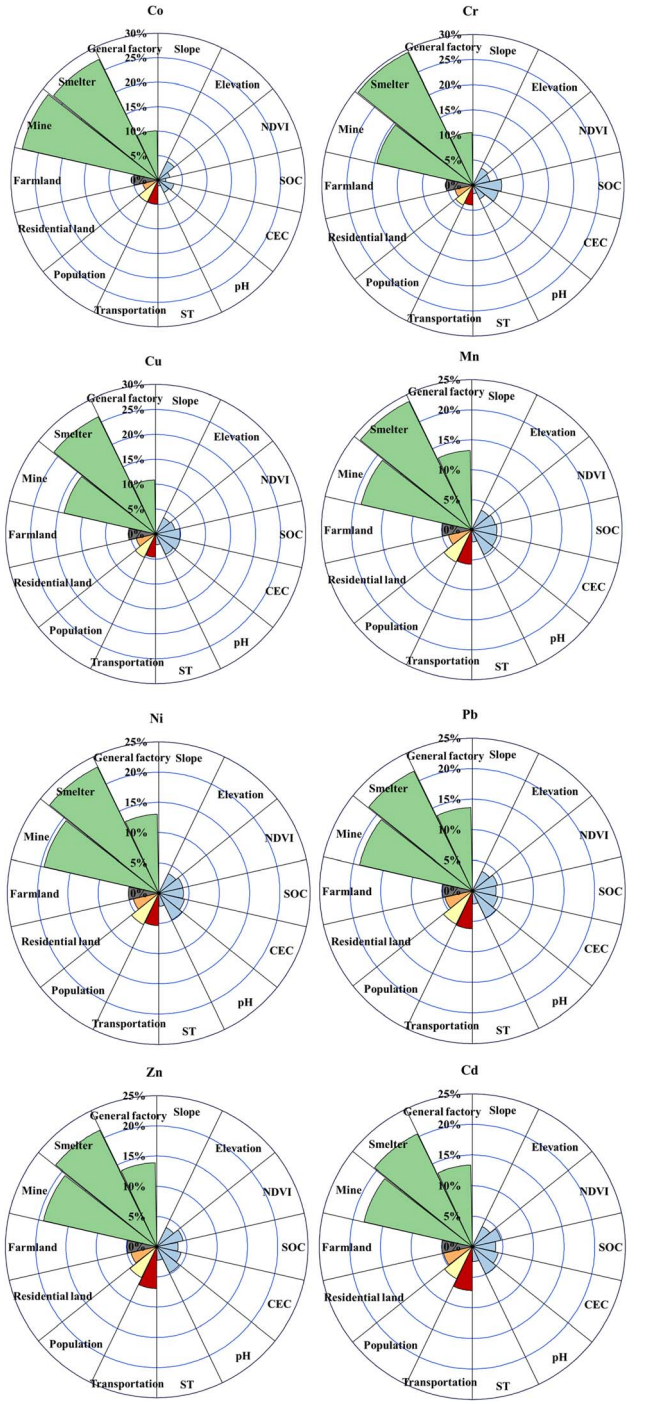

Fig. 6 The relative importance of each environmental factor for soil heavy metal increments. Note: NDVI: normalized difference vegetation index; SOC: soil organic carbon; CEC: cation exchange capacity; ST: soil thickness.

percentages of 56%, 41%, and 3%, respectively. The geo-accumulation risk levels of soil Cu, Pb, and Cd are extremely high, and the average percentages of area contaminated with the three heavy metals are about 78%, 65%, and 78%, respectively. Obviously, the percentages of area with Cu and Pb pollution had a significant increasing trend and rose from 69.65% and 45.29% to 81.21% and 73.78%, respectively.

3.3 Contribution of driving factors for heavy metal increments

The RF model was used to explore the contributions of environmental factors for heavy metal increments for understanding the causes of soil heavy metal pollution changes, and the fitting accuracy of internal 10-fold cross-validation is shown in Table S3.† Except for Cd, the R^2 values of the RF prediction for other elements are larger than 0.7, indicating the higher degree of explanation from these response predictors. The R^2 value for estimating the Cd increment is lower probably because of its observably fragmented distribution and lower increment (Fig. S4†).

The relative importance of different factors for soil heavy metal increments is shown in Fig. 6. The results show that the total contributions of natural factors for Co, Cr, Cu, Mn, Ni, Pb, Zn, and Cd content increment are 16%, 23%, 25%, 24%, 24%, 24%, 24%, and 25%, respectively, and the total contributions of anthropogenic factors are 84%, 77%, 75%, 76%, 76%, 76%, 76%, and 75%, respectively. The first three contributors for these heavy metal increments are the mine, smelter, and factory, and their total contributions are all larger than 50%. Apart from industrial activities, transportation is a large contributor to soil Zn and Cd increments with about 7% contribution, population poses a higher contribution (about 6%) to the soil Pb, Mn, Ni, Zn, and Cd increments, and farmland produces 5% contribution to the soil Cu increment. Compared with human activities, natural factors had an extremely low impact, and soil pH, SOC, and CEC are the three largest natural factors with 4% contribution approximately.

4 Discussion

4.1 Increment of soil heavy metal pollution

From 2016 to 2019, the average ecological risk increased from 127.72 to 136.79, and the total percentage of moderate ecological risk to very high ecological risk rose from 30.68% to 33.96%, which indicated that both the integrated risk degree and high-risk scope from these heavy metals increased. The contents of these heavy metals in more than 50% of the study area increased, and the growth rates of the average content are ranked as Co (65%) > Ni (56%) > Mn (43%) > Pb (40%) > Cr (36%) > Zn (31%) > Cu (23%) > Cd (3%). However, although the soil Co, Cr, and Ni accumulation increased remarkably, they were always at the uncontaminated level in the whole study area, which was probably due to their low background contents. In terms of the contamination areas, soil Cu, Pb, and Zn increased by 12%, 28%, and 17%, respectively, and soil Mn and Cd increased slightly by 2%. Although soil Cd pollution was rather serious, its pollution scope and degree were not intensified, and one possible reason was local soil Cd pollution remediation.[48]

Table S4† shows the Pearson correlations between the soil heavy metal increments. Except for Cd, the increments of other elements have significant correlations, which is because of the more fragmented distribution of the Cd increment. Similar to the spatial pattern of soil heavy metal contents, the higher increments of these heavy metals are mainly distributed in the

central and northern regions (Fig. S4†). The field survey revealed that one smelting and mining site group, and one mining land incorporating quarrying and ore processing are in the central region, and a quarry group and many factories are in the northern region,[47] as shown in Fig. S4.† Many previous studies stated that the heavy metal contents are higher in soils adjacent to industrial lands.[10,47,49] The present study found that both heavy metal contents and their increments in soils near industrial lands are higher.

4.2 Driving forces of soil heavy metal increments

This study utilized the RF regression model to explore the driving forces of soil heavy metal increments, and the prediction accuracy and explanation degree of these entered variables are higher. The results show that the influences of anthropogenic activities are greater than those of natural factors, and industrial activity even poses over 50% contributions for these heavy metal increments. As for Cu, Pb, and Cd with high pollution levels, smelting and mining are the largest contributors, especially for Cu, which is probably because of the long-term discharge of slag, dust, and wastewater.[49–52] Copper smelting and mining in the study area have been operating for more than 60 years and 3000 years.[53,54] Noticeably, many studies ascribed the soil Cr and Ni accumulation to lithogenic sources.[49,55,56] However, the present study found that soil Cr and Ni increments are mainly affected by mining and smelting, which is probably due to the disturbance of slag.[57]

In addition to the industrial activities, population density has a higher contribution to the soil Mn, Ni, Pb, Zn, and Cd increments probably due to the influence of human life activities on pollutant deposition processes.[41,58] The field survey also found that many local residents moved soils from mining regions to plant crops (Fig. S5†), which had a great influence on the soil heavy metal accumulation. Additionally, transportation shows a higher importance for the heavy metal increments, which may be related to the vehicular emissions and ore transportation.[59,60] Overall, these heavy metal increments mainly resulted from the industrial and mining activities in the study area. Thus, properly treating industrial wastes, developing soil remediation in the contaminated region, and managing the reuse of polluted soils are necessary to prevent the aggravation and spread of soil heavy metal pollution.

Notably, in the driving force analysis, land use cannot fully represent the corresponding type of pollution source. For example, farmland is one of the products of agricultural activity, but heavy metal pollution resulting from agricultural activity may be due to the use of fertilizers and pesticides. Therefore, more environmental factors need to be introduced to explore the driving mechanism, which may also improve the simulation accuracy of the RF model. In addition, the present study only explored the contributing sources of soil heavy metal contents, instead of the pollution risk. In fact, exploring the contributing sources of risks can provide more useful information for contamination risk warning, which will be the main work in the future.

5 Conclusion

This study estimated the spatiotemporal distribution of soil heavy metal contents from 2016 to 2019 by using the STOK method, assessed the accumulation risk and potential ecological risk of soil heavy metals, and explored the driving forces for their increments in a typical industrial region in China. The I_{geo} and RI revealed that soil suffered from serious contamination by Cu, Pb, and Cd, and moderate contamination by Zn and Mn; soil pollution of Zn and Mn was extremely low, and more than 30% of areas had moderate to very high potential ecological risk. Overall, higher ecological risk and highly concentrated Cu, Pb, and Cd are mainly distributed in the central and northern areas surrounding various industrial and mining lands. From 2016 to 2019, the accumulations of eight heavy metals in more than 50% of the study area increased; specifically, the pollution scope and degree of Pb, Cu, and Zn increased markedly. Similar to the soil heavy metal contents, their increments in soils near industrial lands were also higher. The RF simulation indicated that the dominant contributors for these eight heavy metal increments were all anthropogenic activities with an average contribution of 77% approximately, especially the industrial and mining activities including smelter (24%), mine (20%), and factory (12%). Accordingly, soil restoration work should focus more on Cu, Pb, and Cd pollution, and more targeted management of industrial activities should be undertaken to control the aggravation of soil heavy metal pollution.

Conflicts of interest

The authors declare that they have no known competing financial interests or personal relationships that could have appeared to influence the work reported in this paper.

Acknowledgements

This research was supported by the National Natural Science Foundation of China (Grant No. 42077378) and the National Key Research and Development Program of China (Grant No. 2018YFC1800104).

References

1 L. Giaccio, D. Cicchella, B. De Vivo, G. Lombardi and M. De Rosa, Does heavy metals pollution affects semen quality in men? A case of study in the metropolitan area of Naples (Italy), *J. Geochem. Explor.*, 2012, **112**, 218–225.
2 Q. Q. Yang, Z. Y. Li, X. N. Lu, Q. N. Duan, L. Huang and J. Bi, A review of soil heavy metal pollution from industrial and agricultural regions in China: Pollution and risk assessment, *Sci. Total Environ.*, 2018, **642**, 690–700.
3 J. Shi, P. Du, H. L. Luo, H. Wu, Y. H. Zhang, J. Chen, M. H. Wu, G. Xu and H. F. Gao, Soil contamination with cadmium and potential risk around various mines in China during 2000-2020, *J. Environ. Manage.*, 2022, **310**, DOI: 10.1016/j.jenvman.2022.114509.

4 Ministry of Environmental Protection of China (MEP), *National Soil Pollution Survey Bulletin*, 2014, in Chinese.
5 Q. Xiao, Y. T. Zong and S. G. Lu, Assessment of heavy metal pollution and human health risk in urban soils of steel industrial city (Anshan), Liaoning, Northeast China, *Ecotoxicol. Environ. Saf.*, 2015, **120**, 377–385.
6 Y. Huang, Q. Q. Chen, M. H. Deng, J. Japenga, T. Q. Li, X. E. Yang and Z. He, Heavy metal pollution and health risk assessment of agricultural soils in a typical peri-urban area in southeast China, *J. Environ. Manage.*, 2018, **207**, 159–168.
7 A. A. Mohammadi, A. Zarei, M. Esmaeilzadeh, M. Taghavi, M. Yousefi, Z. Yousefi, F. Sedighi and S. Javan, Assessment of Heavy Metal Pollution and Human Health Risks Assessment in Soils Around an Industrial Zone in Neyshabur, Iran, *Biol. Trace Elem. Res.*, 2020, **195**, 343–352.
8 S. Y. Wang, Y. B. Zhang, J. L. Cheng, Y. Li, F. Li, Y. Li and Z. Shi, Pollution Assessment and Source Apportionment of Soil Heavy Metals in a Coastal Industrial City, Zhejiang, Southeastern China, *Int. J. Environ. Res. Public Health*, 2022, **19**, DOI: **10.3390/ijerph19063335**.
9 B. Y. Chen, K. L. Liu, Y. L. Liu, J. Qin and Z. H. Peng, Source identification, spatial distribution pattern, risk assessment and influencing factors for soil heavy metal pollution in a high-tech industrial development zone in Central China, *Hum. Ecol. Risk Assess.*, 2021, **27**, 560–574.
10 C. C. Huang, L. M. Cai, Y. H. Xu, L. Jie, L. G. Chen, G. C. Hu, H. H. Jiang, X. B. Xu and J. X. Mei, A comprehensive exploration on the health risk quantification assessment of soil potentially toxic elements from different sources around large-scale smelting area, *Environ. Monit. Assess.*, 2022, **194**, DOI: **10.1007/s10661-022-09804-0**.
11 H. H. Jiang, L. M. Cai, H. H. Wen, G. C. Hu, L. G. Chen and J. Luo, An integrated approach to quantifying ecological and human health risks from different sources of soil heavy metals, *Sci. Total Environ.*, 2020, **701**, DOI: **10.1016/j.scitotenv.2019.134466**.
12 H. H. Jiang, L. M. Cai, G. C. Hu, H. H. Wen, J. Luo, H. Q. Xu and L. G. Chen, An integrated exploration on health risk assessment quantification of potentially hazardous elements in soils from the perspective of sources, *Ecotoxicol. Environ. Saf.*, 2021, **208**, DOI: **10.1016/j.ecoenv.2020.111489**.
13 Y. F. Jiang, Y. C. Ye and X. Guo, Spatiotemporal variation of soil heavy metals in farmland influenced by human activities in the Poyang Lake region, China, *Catena*, 2019, **176**, 279–288.
14 A. Shi, Y. F. Shao, K. L. Zhao and W. J. Fu, Long-term effect of E-waste dismantling activities on the heavy metals pollution in paddy soils of southeastern China, *Sci. Total Environ.*, 2020, **705**, DOI: **10.1016/j.scitotenv.2019.135971**.
15 M. J. He, P. Yan, H. D. Yu, S. Y. Yang, J. M. Xu and X. M. Liu, Spatiotemporal modeling of soil heavy metals and early warnings from scenarios-based prediction, *Chemosphere*, 2020, **255**, DOI: **10.1016/j.chemosphere.2020.126908**.
16 R. Taghizadeh-Mehrjardi, H. Fathizad, M. A. H. Ardakani, H. Sodaiezadeh, R. Kerry, B. Heung and T. Scholten, Spatio-Temporal Analysis of Heavy Metals in Arid Soils at the Catchment Scale Using Digital Soil Assessment and a Random Forest Model, *Remote Sens.*, 2021, **13**, DOI: **10.3390/rs13091698**.
17 G. Christakos, On Certain Classes of Spatiotemporal Random-Fields with Applications to Space-Time Data-Processing, *IEEE Transactions on Systems, Man, and Cybernetics*, 1991, **21**, 861–875.
18 J. X. Wang, M. G. Hu, B. B. Gao, H. M. Fan and J. F. Wang, A spatiotemporal interpolation method for the assessment of pollutant concentrations in the Yangtze River estuary and adjacent areas from 2004 to 2013, *Environ. Pollut.*, 2019, **252**, 501–510.
19 X. Yang, Y. Yang, K. Li and R. J. Wu, Estimation and characterization of annual precipitation based on spatiotemporal kriging in the Huanghuaihai basin of China during 1956-2016, *Stoch. Environ. Res. Risk Assess.*, 2020, **34**, 1407–1420.
20 Y. Yang, H. Li, S. D. Deng, X. Yang, M. X. Wang, W. F. Tan, Z. Y. Wu, Q. L. Wang and Y. Z. Zhou, Prediction and analysis of the soil organic matter distribution with the spatiotemporal kriging method, *Earth Science Informatics*, 2022, **15**, 1621–1633.
21 S. J. Li, L. Yang, L. D. Chen, F. K. Zhao and L. Sun, Spatial distribution of heavy metal concentrations in peri-urban soils in eastern China, *Environ. Sci. Pollut. Res.*, 2019, **26**, 1615–1627.
22 P. W. Qiao, S. C. Yang, M. Lei, T. B. Chen and N. Dong, Quantitative analysis of the factors influencing spatial distribution of soil heavy metals based on geographical detector, *Sci. Total Environ.*, 2019, **664**, 392–413.
23 H. Z. Wang, Q. Yilihamu, M. N. Yuan, H. T. Bai, H. Xu and J. Wu, Prediction models of soil heavy metal(loid)s concentration for agricultural land in Dongli: A comparison of regression and random forest, *Ecol. Indic.*, 2020, **119**, DOI: **10.1016/j.ecolind.2020.106801**.
24 L. Breiman, Random forests, *Mach. Learn.*, 2001, **45**, 5–32.
25 Z. W. Su, L. Lin, Y. M. Chen and H. H. Hu, Understanding the distribution and drivers of PM2.5 concentrations in the Yangtze River Delta from 2015 to 2020 using Random Forest Regression, *Environ. Monit. Assess.*, 2022, **194**, DOI: **10.1007/s10661-022-09934-5**.
26 G. X. Huang, X. H. Wang, D. Chen, Y. P. Wang, S. X. Zhu, T. Zhang, L. Liao, Z. Tian and N. Wei, A hybrid data-driven framework for diagnosing contributing factors for soil heavy metal contaminations using machine learning and spatial clustering analysis, *J. Hazard. Mater.*, 2022, **437**, DOI: **10.1016/j.jhazmat.2022.129324**.
27 G. Christakos, *Random Field Models in Earth Sciences*, Academic Press, San Diego, 1992.
28 P. Y. Zhang, C. Z. Qin, X. Hong, G. H. Kang, M. Z. Qin, D. Yang, B. Pang, Y. Y. Li, J. J. He and R. P. Dick, Risk assessment and source analysis of soil heavy metal pollution from lower reaches of Yellow River irrigation in China, *Sci. Total Environ.*, 2018, **633**, 1136–1147.
29 W. Wu, P. Wu, F. Yang, D. L. Sun, D. X. Zhang and Y. K. Zhou, Assessment of heavy metal pollution and human health risks in urban soils around an electronics manufacturing facility, *Sci. Total Environ.*, 2018, **630**, 53–61.

30 M. A. H. Bhuiyan, S. C. Karmaker, M. Bodrud-Doza, M. A. Rakib and B. B. Saha, Enrichment, sources and ecological risk mapping of heavy metals in agricultural soils of dhaka district employing SOM, PMF and GIS methods, *Chemosphere*, 2021, **263**, DOI: 10.1016/j.chemosphere.2020.128339.
31 China National Environmental Monitoring Center (CNEMC), *The Background Centrations of Soil Elements of China*, China Environmental Science Press, Beijing, China, 1990, in Chinese.
32 G. Müller, Index of geoaccumulation in sediments of the Rhine River, *Geojournal*, 1969, **2**, 108–118.
33 L. Hakanson, An Ecological Risk Index for Aquatic Pollution-Control - a Sedimentological Approach, *Water Res.*, 1980, **14**, 975–1001.
34 Y. Li, Z. Dong, D. K. Feng, X. M. Zhang, Z. Y. Jia, Q. B. Fan and K. Liu, Study on the risk of soil heavy metal pollution in typical developed cities in eastern China, *Sci. Rep.*, 2022, **12**, DOI: 10.1038/s41598-022-07864-3.
35 Z. Q. Xu, S. Ni, X. G. Tuo and C. J. Zhang, Calculation of heavy metal's toxicity coefficient in the evaluation of Potential Ecological Risk Index, *Environ. Sci. Technol.*, 2008, **31**, 112–115in Chinese.
36 Q. Y. Guan, R. Zhao, F. F. Wang, N. H. Pan, L. Q. Yang, N. Song, C. Q. Xu and J. K. Lin, Prediction of heavy metals in soils of an arid area based on multi-spectral data, *J. Environ. Manage.*, 2019, **243**, 137–143.
37 A. Król, K. Mizerna and M. Bozym, An assessment of pH-dependent release and mobility of heavy metals from metallurgical slag, *J. Hazard. Mater.*, 2020, **384**, DOI: 10.1016/j.jhazmat.2019.121502.
38 Y. A. Yobouet, K. Adouby and P. Drogui, Experimental Methodology to Assess Retention of Heavy Metals Using Soils from Municipal Waste Landfills, *Water, Air, Soil Pollut.*, 2016, **227**, DOI: 10.1007/s11270-015-2706-x.
39 Q. Ding, G. Cheng, Y. Wang and D. F. Zhuang, Effects of natural factors on the spatial distribution of heavy metals in soils surrounding mining regions, *Sci. Total Environ.*, 2017, **578**, 577–585.
40 Z. Y. Li, Z. W. Ma, T. J. van der Kuijp, Z. W. Yuan and L. Huang, A review of soil heavy metal pollution from mines in China: Pollution and health risk assessment, *Sci. Total Environ.*, 2014, **468**, 843–853.
41 R. Liu, M. E. Wang, W. P. Chen and C. Peng, Spatial pattern of heavy metals accumulation risk in urban soils of Beijing and its influencing factors, *Environ. Pollut.*, 2016, **210**, 174–181.
42 T. J. Song, X. S. Su, J. He, Y. K. Liang and T. Zhou, Source apportionment and health risk assessment of heavy metals in agricultural soils in Xinglonggang, Northeastern China, *Hum. Ecol. Risk Assess.*, 2018, **24**, 509–521.
43 S. N. Hou, N. Zheng, L. Tang, X. F. Ji, Y. Y. Li and X. Y. Hua, Pollution characteristics, sources, and health risk assessment of human exposure to Cu, Zn, Cd and Pb pollution in urban street dust across China between 2009 and 2018, *Environ. Int.*, 2019, **128**, 430–437.
44 C. Peng, Z. Y. Ouyang, M. E. Wang, W. P. Chen, X. M. Li and J. C. Crittenden, Assessing the combined risks of PAHs and metals in urban soils by urbanization indicators, *Environ. Pollut.*, 2013, **178**, 426–432.
45 X. Y. Zhang, Y. Y. Sui, X. D. Zhang, K. Meng and S. J. Herbert, Spatial variability of nutrient properties in black soil of northeast China, *Pedosphere*, 2007, **17**, 19–29.
46 Y. Yang, X. Yang, M. J. He and G. Christakos, Beyond mere pollution source identification: Determination of land covers emitting soil heavy metals by combining PCA/APCS, GeoDetector and GIS analysis, *Catena*, 2020, **185**, DOI: 10.1016/j.catena.2019.104297.
47 X. Yang, Y. Yang, Y. Y. Wan, R. J. Wu, D. K. Feng and K. Li, Source identification and comprehensive apportionment of the accumulation of soil heavy metals by integrating pollution landscapes, pathways, and receptors, *Sci. Total Environ.*, 2021, **786**, DOI: 10.1016/j.scitotenv.2021.147436.
48 Y. H. Gong, K. Pi, D. M. Li and Y. Y. Gong, Selection of remediation technologies for heavy metal contaminated farmland around the mining area and the existing problems - Taking the project of soil remediation in heavy metal contaminated farmland in Jinhu, Daye City, Hubei Province as an example, *2016 Annual Academic Meeting Proceedings for the Sixth Seminar on Heavy Metal Pollution Prevention and Risk Assessment and the Professional Committee on Heavy Metal Pollution Prevention and Control*, Xiamen, Fujian, China, 2016, in Chinese.
49 L. Hua, X. Yang, Y. J. Liu, X. L. Tan and Y. Yang, Spatial Distributions, Pollution Assessment, and Qualified Source Apportionment of Soil Heavy Metals in a Typical Mineral Mining City in China, *Sustainability*, 2018, **10**, DOI: 10.3390/su10093115.
50 Y. N. Hu and H. F. Cheng, Application of Stochastic Models in Identification and Apportionment of Heavy Metal Pollution Sources in the Surface Soils of a Large-Scale Region, *Environ. Sci. Technol.*, 2013, **47**, 3752–3760.
51 Y. N. Hu, K. L. He, Z. H. Sun, G. Chen and H. F. Cheng, Quantitative source apportionment of heavy metal(loid)s in the agricultural soils of an industrializing region and associated model uncertainty, *J. Hazard. Mater.*, 2020, **391**, DOI: 10.1016/j.jhazmat.2020.122244.
52 Y. H. Li, H. F. Kuang, C. H. Hu and G. Ge, Source Apportionment of Heavy Metal Pollution in Agricultural Soils around the Poyang Lake Region Using UNMIX Model, *Sustainability*, 2021, **13**, DOI: 10.3390/su13095272.
53 L. M. Cai, Z. C. Xu, J. Y. Qi, Z. Z. Feng and T. S. Xiang, Assessment of exposure to heavy metals and health risks among residents near Tonglushan mine in Hubei, China, *Chemosphere*, 2015, **127**, 127–135.
54 L. M. Cai, Q. S. Wang, J. Luo, L. G. Chen, R. L. Zhu, S. Wang and C. H. Tang, Heavy metal contamination and health risk assessment for children near a large Cu-smelter in central China, *Sci. Total Environ.*, 2019, **650**, 725–733.
55 Y. N. Hu, X. P. Liu, J. M. Bai, K. M. Shih, E. Y. Zeng and H. F. Cheng, Assessing heavy metal pollution in the surface soils of a region that had undergone three decades of intense industrialization and urbanization, *Environ. Sci. Pollut. Res.*, 2013, **20**, 6150–6159.

56 J. Zhou, K. Feng, Z. P. Pei, F. Meng and J. Sun, Multivariate analysis combined with GIS to source identification of heavy metals in soils around an abandoned industrial area, Eastern China, *Ecotoxicology*, 2016, **25**, 380–388.
57 Y. Jafari, B. G. Jones, J. C. Pacheco and S. Umoru, Trace element soil contamination from smelters in the Illawarra region, New South Wales, Australia, *Environ. Earth Sci.*, 2020, **79**, DOI: **10.1007/s12665-020-09115-y**.
58 X. H. Xia, X. Chen, R. M. Liu and H. Liu, Heavy metals in urban soils with various types of land use in Beijing, China, *J. Hazard. Mater.*, 2011, **186**, 2043–2050.
59 S. De Silva, A. S. Ball, T. Huynh and S. M. Reichman, Metal accumulation in roadside soil in Melbourne, Australia: Effect of road age, traffic density and vehicular speed, *Environ. Pollut.*, 2016, **208**, 102–109.
60 Z. W. Ma, K. Chen, Z. Y. Li, J. Bi and L. Huang, Heavy metals in soils and road dusts in the mining areas of Western Suzhou, China: a preliminary identification of contaminated sites, *J. Soils Sediments*, 2016, **16**, 204–214.

